REPORT DOCUMENTATION PAGE

AFRL-SR-AR-TR-03-

0080

Public reporting burden for this collection of information is estimated to average 1 hour per response, including the time for reviewing instru data needed, and completing and reviewing this collection of information. Send comments regarding this burden estimate or any other asp this burden to Department of Defense, Washington Headquarters Services, Directorate for Information Operations and Reports (0704-018 4302. Respondents should be aware that notwithstanding any other provision of law, no person shall be subject to any penalty for failing t valid OMB control number. PLEASE DO NOT RETURN YOUR FORM TO THE ABOVE ADDRESS.

1. REPORT DATE (DD-MM-YYYY)	2. REPORT TYPE	3. DATES COVERED
28-02-2003	Final Report	01-12-1999 to 31-11-2002

4. TITLE AND SUBTITLE
Physical Chemistry of Energetic Nitrogen Compounds

5a. CONTRACT NUMBER

5b. GRANT NUMBER
F49620-00-1-0062

5c. PROGRAM ELEMENT NUMBER
61102F

6. AUTHOR(S)
Robert D. Coombe

5d. PROJECT NUMBER
2303

5e. TASK NUMBER
EX

5f. WORK UNIT NUMBER

7. PERFORMING ORGANIZATION NAME(S) AND ADDRESS(ES)
Department of Chemistry and Biochemistry
University of Denver
2190 East Iliff Avenue
Denver, CO 80208

8. PERFORMING ORGANIZATION REPORT NUMBER

9. SPONSORING / MONITORING AGENCY NAME(S) AND ADDRESS(ES)
AFOSR/NL
4015 Wilson Blvd., Rm. 713
Arlington, VA 22203-1954

10. SPONSOR/MONITOR'S ACRONYM(S)

11. SPONSOR/MONITOR'S REPORT NUMBER(S)

12. DISTRIBUTION / AVAILABILITY STATEMENT

Approve for Public Release: Distribution Unlimited

13. SUPPLEMENTARY NOTES

14. ABSTRACT Photolysis of nitrogen trichloride at 193 nm efficiently produces the excited singlet delta state of NCl, a species useful as an energy carrier in atomic iodine lasers. Photolysis of mixtures of nitrogen trichloride with molecular iodides at 193 nm produces strong emission at 1315 nm from excited iodine atoms. Rate constants for the collisional quenching of excited singlet delta NCl and excited iodine atoms by nitrogen trichloride were determined at room temperature. In a second part of the research, the deposition of BN films from the dissociation of boron triazide was investigated using plasma-assisted deposition methods. These experiments produced stable, dense, and adherent BN films with good chemical characteristics. The films were found to be amorphous, though, a result thought to be associated with self-assembly of boron triazide dissociation fragments into BN nanoparticles in the gas phase. This hypothesis was supported by IR analysis of the constituents of a boron triazide/argon plasma trapped in a low temperature matrix.

15. SUBJECT TERMS

16. SECURITY CLASSIFICATION OF:			17. LIMITATION OF ABSTRACT	18. NUMBER OF PAGES	19a. NAME OF RESPONSIBLE PERSON
a. REPORT	b. ABSTRACT	c. THIS PAGE			Robert D. Coombe
unclassified	unclassified	unclassified		24	19b. TELEPHONE NUMBER (include area code) 303-871-2966

20030326 008

EXECUTIVE SUMMARY

The storage of energy in molecules and the dynamics of chemical processes by which it may released are important issues for a number of applications of interest to the scientific community and the U.S. Air Force. This report describes the results of a three year research program that investigated energetic azides and amines, and the possible utility of these chemical systems in (1) chemical lasers and (2) low energy deposition processes for thin films of group III nitrides.

In the first part of the work, the photochemistry and reactions of the energetic molecule NCl_3 were explored with a view to the production of excited $NCl(a^1\Delta)$. $NCl(a^1\Delta)$ is a metastable excited species that has been shown to efficiently transfer its energy to iodine atoms, and both pulsed and cw iodine lasers operating at 1315 nm have been demonstrated based on this process. These devices have been given the name AGIL, for all gas phase iodine laser. In the present work, one project explored the photochemistry of NCl_3. The UV absorption spectrum of the molecule was measured from 170 – 300 nm, and pulsed photolysis experiments were performed using laser sources at 193 and 249 nm. Photolysis at 193 nm was found to produce $NCl(a^1\Delta)$ with a quantum yield of 0.8 ± 0.2. No evidence was found of the operation of other dissociation channels that might produce excited NCl_2 or Cl_2. When the photolytic iodine atom source CH_2I_2 was added to the gas mixture, strong emission from excited $I^*(5^2P_{1/2})$ was produced, evidence of the operation of the energy transfer process noted above. These data suggest that this system might readily be used to demonstrate a photochemical I* laser, but this would require the generation of greater densities of gaseous NCl_3 than those employed in the current experiments. Photolysis of NCl_3 at 249 nm was found to produce no excited NCl. Instead, strong emission from a series of bands in the visible and near IR region was observed, and these features are tentatively assigned to transitions in NCl_2.

A second project was directed toward the measurement of rate constants for the quenching of $NCl(a^1\Delta)$ and I* by collsions with NCl_3 and its photofragments. For measurements of the quenching of $NCl(a^1\Delta)$, flowing mixtures of NCl_3 in Ar diluent were photolyzed at 193 nm, generating $NCl(a^1\Delta)$ as above. Time profiles of the decay of the excited NCl were recorded for a range of NCl_3 densities, and the value of the quenching rate constant was determined from plots of the observed decay rate vs. the NCl_3 density. The value of the rate constant for quenching of $NCl(a^1\Delta)$ by NCl_3 was determined to be $k_1 = (3.4 \pm 1.7) \times 10^{-13}$ cm^3s^{-1} at room temperature. Measurements of the rate constant for I* quenching by NCl_3 were made by photolysis of mixtures of NCl_3 and CF_3I in Ar diluent. Photolysis of CF_3I at this wavelength is known to efficiently produce I*, and no excited $NCl(a^1\Delta)$ is produced by the photolysis of NCl_3 as noted above. Measurements of the time decay of 1315 nm emission from I* were made for a range of NCl_3 densities, and the I* quenching rate constant obtained from the data is $k_2 = (9.5 \pm 2.0) \times 10^{-13}$ cm^3s^{-1}. Neither k_1 nor k_2 were found to vary with the fluence of the laser, i.e., with the density of NCl_3 photofragments. In particular, 249 nm photolysis of NCl_3 is expected to produce NCl_2 radicals (as noted above) and Cl atoms. Chlorine atoms are known to be efficient quenchers of I*, and the absence of a fluence dependence suggests that they are rapidly

removed from the system, either by loss at the cell walls or by reaction with the parent NCl_3.

The second part of the research program was directed toward investigation of the energetic molecule boron triazide, $B(N_3)_3$, as a precursor for boron nitride thin films. This species is very attractive as a source of BN because of its chemical composition (containing only boron and nitrogen) and its energy content. In work done in our laboratory under the aegis of a previous AFOSR grant, a simple gas phase synthesis of $B(N_3)_3$ was developed and the molecule was shown be useful for the deposition of BN films by either thermal dissociation or dissociation in collisions with $N_2(A^3\Sigma_u^+)$ metastables. Although the films produced had good chemical composition, they degraded rapidly in room air and adhered poorly to the Si substrates used. The focus of the present work was deposition of higher quality films. Plasma-assisted deposition was investigated for this purpose, with good results. BN films deposited on Si and sapphire substrates exhibited very good chemical composition, high density, good adhesion, and stability. Plasma-deposited films showed no evidence of chemical degradation after exposure to room air for 5 months. The films produced all had hexagonal structure, even under higher energy conditions that should favor generation of cubic (diamond-like) BN, and on single crystal Ni substrates that have an excellent lattice match with c-BN.

Plasma-deposited films from $B(N_3)_3$ were also fund to be amorphous. In an effort to understand this result, both experimental and theoretical methods were employed in an investigation of the molecular mechanism of film deposition. The principal stable product of $B(N_3)_3$ dissociation in the gas phase has been shown to be linear NNBN, a molecule isoelectronic to cyanogen. It has been speculated that self-assembly of NNBN into six-member BN ring structures may underlie the hexagonal structure of the films observed, and indeed computations performed in our laboratory of the potential energy paths associated with this self assembly process supported this hypothesis. In the present work, these computations (using DFT methods at the B3LYP/6-31g* level) were extended to determination of the vibrational frequencies and IR intensities of several B_3N_x ring structures. The highest intensity features of all of the ring structures were located near 1640 cm^{-1}, and correlated with B-N ring stretching vibrations. Experiments were performed in an effort to identify these BN ring species in a discharge through gaseous $B(N_3)_3$/Ar mixtures that simulated the film deposition conditions. A small portion of the flow was passed through a pinhole and condensed on the cold surface (10 K) of a substrate in a low temperature matrix isolation apparatus. The results of these experiments showed the growth of the 1640 cm^{-1} feature only when the discharge was on, strongly supporting the notion that six-membered BN ring structures are generated in the gas phase. If this is indeed the case, then this gas phase chemistry dominates the physical structure (and indeed the chemical composition) of the BN films that are deposited in the plasma-deposition apparatus.

The major conclusions of this work are that the NCl_3 system remains a very good candidate for a high energy AGIL device. The data generated in the present work indicate that this system is compatible with the excitation of I* at densities on the order of 10^{14} cm^{-3}, more than an order of magnitude greater than the densities of previous discharge-flow investigations of this system. The results bode well for further scaling of a cw device, and for demonstration of a pulsed I* laser based on NCl_3 photodissociation. With regard to the BN work, there is little doubt that $B(N_3)_3$ is an excellent source for BN

films. The principal issue appears to be separation of the gas phase chemistry, dominated by self-assembly of NNBN fragments into hexagonal ring structures, from growth of the film on the substrate surface. Indeed, the future for this work may well lie in the generation of BN nanoparticles, as these would appear to be the result of the gas phase self assembly processes in the system.

To date, two publications have arisen from this work. These are:

1. K.R. Hobbs and R.D. Coombe, "Plasma-Assisted Deposition of BN Thin Films from $B(N_3)_3$", Thin Solid Films, **402**, 162 (2002).

2. R.D. Coombe, J.V. Gilbert, S.P. Beaton, and N. Mateljevic, "Photodissociation of NCl_3 at 193 nm and 249 nm", J. Phys. Chem. A, **106**, 8422 (2002)

A manuscript describing the work on $NCl(a^1\Delta)$ and I* quenching is in preparation. Much of the work on the deposition of BN films was done by Keith R. Hobbs, a graduate student who completed his doctoral degree at the University of Dénver in 2001. The title of Dr. Hobbs' thesis is "Boron Triazide for Deposition of BN Films".

The principal investigator for this research program was Professor Robert D. Coombe. Other persons who made significant contributions included Professor Julanna V. Gilbert (a faculty member in the Chemistry and Biochemistry department at the University of Denver), Dr. Stuart P. Beaton (a postdoctoral research associate), Dr. Keith R. Hobbs (the doctoral student noted above), Ms. Natasa Mateljevic (a graduate student), and Mr. John Glennon (an undergraduate student).

INTRODUCTION AND OBJECTIVES

This report describes the results of a three-year program of basic research directed toward understanding the chemical behavior of small, energetic nitrogen-containing compounds, particularly azides and amines. The research, which grew from many years of previous work in our laboratory, was focused on two particular areas of application. These are the potential utility of these compounds (or their fragments or derivatives) as energy carriers in chemically pumped laser systems, and as chemical precursors for the low-energy deposition of nitride thin films.

Chemical lasers, first demonstrated in the 1960's, are still the highest power and most efficient of high-energy cw laser devices. The U.S. Air Force has many potential applications for chemical lasers, at a host of wavelengths and power levels. The shortest wavelength high-energy chemical laser is the COIL, or chemical oxygen-iodine laser, first developed[1] during the 1970's. While COIL is surely capable of high energies and efficiencies and its 1315 nm wavelength is ideal for atmospheric transmission, it suffers from the two phase (liquid-gas) chemistry[2] used to produce the energy carrier, metastable excited $O_2(a^1\Delta)$. In recent years there has been considerable interest in the development of an all gas-phase chemical iodine laser, or AGIL. This work has focused principally on excitation of iodine atoms by collisions with metastable excited $NCl(a^1\Delta)$, a species that can be produced by gas phase reactions involving either azides[3] or amines[4]. An iodine laser based on pulsed generation of $NCl(a^1\Delta)$ from photodissociation of ClN_3 was first demonstrated[5] in our laboratory in 1995. This was followed by the demonstration of a cw laser device[6] (the first true AGIL) based on the generation of excited NCl from the Cl + N_3 reaction at the Air Force Research Laboratory in 2000. Since that time, researchers at AFRL have continued to work on scaling this azide-based AGIL device. In our laboratory, our attention turned to an alternative source of $NCl(a^1\Delta)$ based on amine chemistry. In experiments performed in the early 1990's, it had been shown[4] that the reaction of NCl_3 with excess hydrogen atoms is an efficient source of excited NCl, by the following mechanism:

$$H + NCl_3 \rightarrow NCl_2 + HCl \qquad (1)$$

$$H + NCl_2 \rightarrow NCl(a^1\Delta) + HCl \qquad (2)$$

Addition of HI to this reaction mixture, such that iodine atoms are produced by the H + HI reaction[7], results in the efficient conversion of energy stored in the $NCl(a^1\Delta)$ present in the mixture into excitation of $I(5^2P_{1/2})$, the 1315 nm emitter[8]. The present research has been directed toward the evaluation of the potential of this system for pumping a high-energy laser device. The results presented below describe the measurement of a number of key parameters in the complex kinetics of this system and first efforts at scaling in a system initiated by pulsed photolysis.

The second research area involves the deposition of thin nitride films, in particular thin films of group III nitrides. The normal means used for the deposition of such films (e.g., plasma deposition or chemical vapor deposition) all involve the input of significant amounts of energy of one form or another. These high energies are needed to initiate and carry the chemical reactions that generate the film constituents. For example, ammonia

(NH_3) is used as the nitrogen source for many nitride films[9], and significant amounts of energy are needed to break its very strong NH bonds. CVD processes for deposition of nitrides from ammonia are typically operated at temperatures of several hundred degrees[10]. These high temperatures can adversely affect the characteristics of the films produced. For some tertiary nitrides, the films themselves are not stable at the high temperatures needed to drive the ammonia-based chemistry[11]. These difficulties have generated considerable interest in the use of energetic alternatives to NH_3 in these systems, and much of this interest has been focused on azides and hydrazines. In 1995, a novel synthesis for the energetic compound boron triazide ($B(N_3)_3$) was discovered in our laboratory[12]. This very unique compound, containing only boron and nitrogen, is in many ways an ideal precursor for the deposition of films of boron nitride (BN). Since BN is isoelectronic to carbon, its films have properties similar to carbon films with either hexagonal or cubic (diamond-like) structures[13]. No good synthesis for pure cubic BN is known, and this has been a goal of researchers in this field for many years. Further interest in this area has been fueled in the last decade by the tremendous growth of research on GaN films.

The present research focused on the development of an effective means for the deposition of BN films from $B(N_3)_3$. Previous research in our laboratory had demonstrated the deposition of BN from both the thermal dissociation of $B(N_3)_3$ and the dissociation of this azide in collisions with excited metastable N_2 molecules[14]. The films produced were amorphous, though, and subject to rapid degradation. In the research presented below, plasma dissociation of $B(N_3)_3$ was investigated as a means for deposition of BN. Further, an investigation of the molecular mechanism of film formation was performed using a combination of experimental and theoretical methods.

These research efforts have resulted in a number of publications in the literature and in continued research in our own laboratory and elsewhere. In particular, research on the amine/I* system is continuing in several laboratories under the aegis of a multi-university research initiative (MURI) grant from the Air Force Office of Scientific Research[15].

RESULTS OF THE PROGRAM

Part I. Amine Chemistry for the Production of $I^*(5^2P_{1/2})$

Although the initial demonstration of the $NCl(a^1\Delta)/I^*$ laser[5] in our laboratory was performed with a ClN_3-based system and the cw AGIL device[6] demonstrated at Kirtland AFB is based on $Cl + N_3$ chemistry, it has always been our belief that amine systems hold greater promise than azides for scaling to high energies. The research projects described below are directed toward an initial test of this hypothesis by the production of higher densities of reagents in pulsed systems.

1. Photochemistry of NCl_3

Photolysis of NCl_3, a weakly bound energetic molecule, produces a singlet excited state that can dissociate to singlet, doublet, or triplet fragments as follows:

$$NCl_3 + h\nu \rightarrow NCl^* \quad (3)$$

$$NCl_3^* \rightarrow NCl(a^1\Delta, b^1\Sigma^+) + Cl_2(X^1\Sigma_g^+) \quad (4)$$

$$NCl_3^* \rightarrow NCl_2 \text{ (doublet states)} + Cl(^2P) \quad (5)$$

$$NCl_3^* \rightarrow NCl\ (X^3\Sigma^-) + Cl_2(^3\Pi) \quad (6)$$

Very little experimental information about the photochemistry of NCl_3 was available prior to the present work. An exception was research performed in our laboratory in the late 1980's that focused on photolysis of this molecule at the 249 and 308 nm excimer laser wavelengths[16]. The principal result of these experiments was the observation of strongly banded emission in the visible region that was thought to arise from excited states of NCl_2 or NCl_3. In the present work, we extended these results farther into the visible and near infrared.

The experimental methods employed in these experiments have been described in detail in the literature[4,8,17]. NCl_3 was generated in a shielded apparatus in a fume hood by passage of gaseous Cl_2 through an acidified aqueous solution of $(NH_4)_2SO_4$. The NCl_3 was collected in a trap at 193K. Any Cl_2 condensed in the trap along with the NCl_3 was removed by warming to room temperature and entrainment in a stream of Ar. For the experiments described below, the liquid NCl_3 remaining in the trap at room temperature was entrained in a flow of argon at atmospheric pressure, with the flow returning to the hood exhaust. The proportion of NCl_3 in this atmospheric pressure NCl_3/Ar flow was determined by absorbance of 254 nm radiation from a low pressure Hg lamp. Small flows of the NCl_3/Ar mixture were metered out of the atmospheric pressure stream into the photolysis cell used for the experiments. The cell was constructed from a stainless steel block with 2.54 cm diameter channels for flow of the gases, the passage of the photolysis laser beam, and the observation of emissions from the photolysis zone. Pulsed radiation from the photolysis laser entered the cell via 15 cm long side-arms that were baffled to reduce the effects of light scattering. Emission from the cell in the near IR region was observed with an intrinsic Ge detector cooled to 77 K and equipped with appropriate narrow-band filters, or by transmitting the emission via an optical fiber to a 0.25 m monochromator that dispersed the emission before its detection. Emission in the visible region was detected with a cooled GaAs photomultiplier tube. Spectra of pulsed emissions were recorded using a boxcar integrator, and time profiles of the emissions were recorded with a digital oscilloscope.

Figure 1 shows the spectrum of emission from the pulsed photolysis of NCl_3 at 249 nm, recorded between 750 and 1400 nm. This beautiful band system is an extension of that reported by Gilbert and co-workers[16] in 1987. Its intensity was observed to vary linearly with the fluence of the photolysis laser throughout the spectral region shown in the figure, and the time profile of the emission exhibited a risetime limited by the detector used in the experiments (a cooled Ge detector with a 13 μs time constant) followed by a decay over 50 μs. These results suggest that the emitter is a product of the single photon dissociation of the parent NCl_3, most probably NCl_2 formed by the double channel reaction (5) above. There is no evidence of emission from either excited $Cl_2(^3\Pi)$ or

$NCl(a^1\Delta)$, suggesting that the singlet and triplet channels (reactions 5 and 6, respectively) are not operative at this photolysis wavelength.

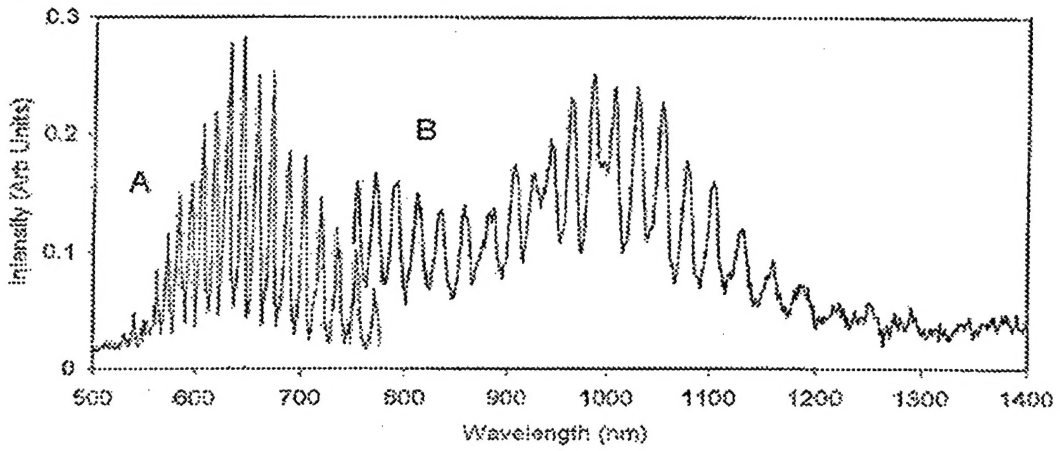

Figure 1. Spectrum of visible and near IR emission produced from the 249 nm photolysis of NCl_3, gated from 0 to 50 μs. (A) data from Gillbert, et. al. (ref. 16); (B) present data.

In the present research, we also investigated the photolysis of NCl_3 at 193 nm. The first part of this work involved measurement of the absorption spectrum of the molecule in this region, which was unknown. Clark and Clyne[18] reported the absorption spectrum in the UV region, but only for wavelengths above 210 nm. We used a VUV spectrometer equipped with a deuterium lamp and modified to incorporate a 1.0 cm absorption cell to extend the spectrum down to 170 nm. The result, shown in Figure 2, indicates that the very strong absorption feature with a maximum at 220 nm extends well below 200 nm. From our measurement of the density of NCl_3 present in the cell (from the absorbance at 254 nm and the absorption cross section at that wavelength reported by Clark and Clyne[18]), the absorption cross section at 193 nm is determined to be 4.5×10^{-18} cm^2.

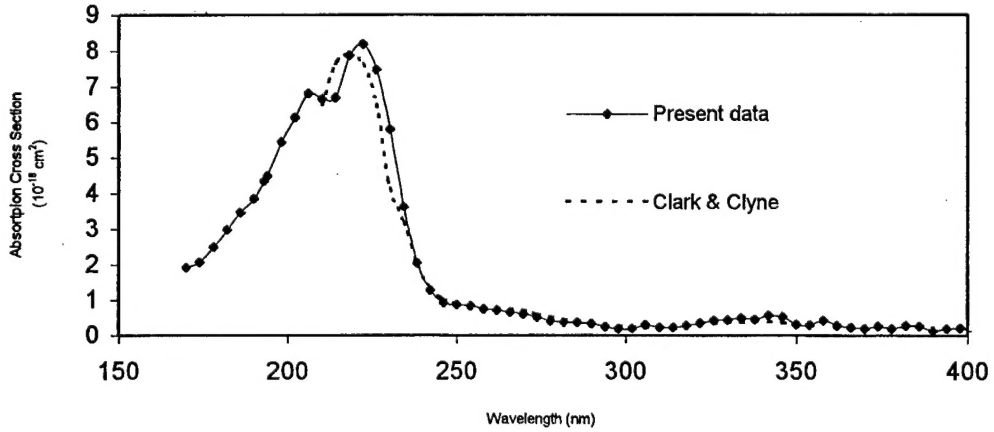

Figure 2. UV/VUV absorption spectrum of NCl_3. Present data are compared with earlier measurement by Clark and Clyne (ref. 18)

Pulsed photolysis of NCl_3 with the output from an ArF excimer laser at 193 nm resulted in emission from photofragments in both the visible and near IR regions. Figure 3 shows the spectrum of emission in the visible, easily identified as sequences of the $b^1\Sigma^+ \rightarrow X^3\Sigma^-$ transition[19] in NCl. The intensities of the $\Delta v = \pm 1,2$, and 3 sequences indicate that electronically excited NCl is also produced with considerable vibrational excitation[20]. The time profile of the emission from the v=0 vibrational level indicates an electronics-limited rise followed by a longer rise over hundreds of μs that is likely associated with population of v=0 by cascade from higher vibrational levels, followed by a slow decay over a few ms. Emission in the near IR at 1077 nm from $NCl(a^1\Delta)$ was also observed, and its time profile is shown in Figure 4. Here again, the detector-limited rise suggests that the excited NCl is a direct photolysis product. The intensities of emissions from both the $a^1\Delta$ and $b^1\Sigma^+$ states of NCl were observed to vary linearly with the fluence of the photolysis laser. Clearly, the singlet dissociation channel (reaction 4) is operative for 193 nm photodissociation. Further, no emission was observed from excited NCl_2 (as in Figure 1) or Cl_2, suggesting that the doublet and triplet channels are closed at this wavelength.

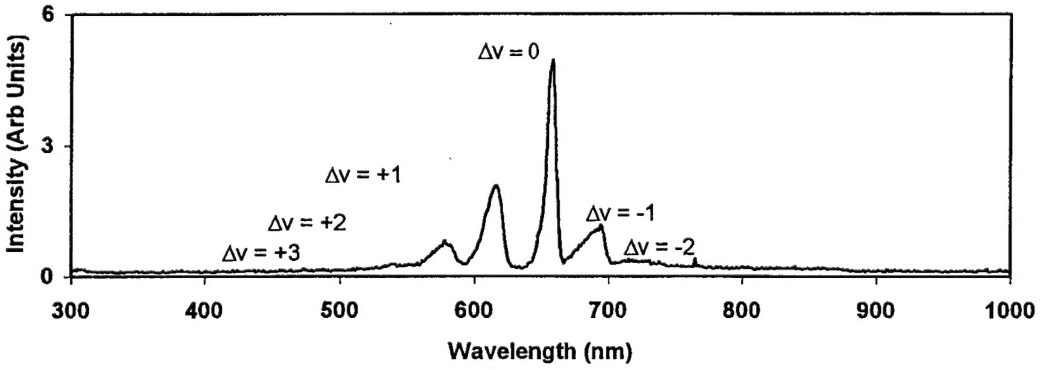

Figure 3. Spectrum of visible emission resulting from the photolysis of NCl_3 at 193 nm. Sequences of the NCl b→X transition are labeled.

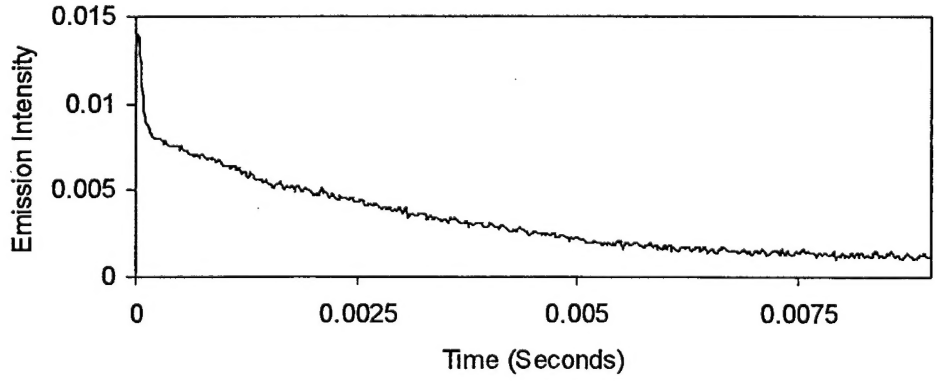

Figure 4. Time profile of $NCl(a^1\Delta)$ emission observed from photolysis of NCl_3 at 193 nm.

Excited singlet NCl is produced when NCl_3 is photolyzed at 193 nm. Iodine atoms can be introduced when CH_2I_2 (a known[21] iodine source at 193 nm) is added to the gas flow. Figure 5 shows time profiles of 1315 nm emission from $I^*(5^2P_{1/2})$ produced from 193 nm photolysis of mixtures of NCl_3, CH_2I_2, and Ar. Data for three experimental conditions (representing different densities of photoproducts) are shown. For each set of data, the bottom trace is a baseline obtained from photolysis of Ar alone, the middle trace was obtained from photolysis of CH_2I_2/Ar, and the top trace was obtained from photolysis of NCl_3/CH_2I_2/Ar. Photolysis of CH_2I_2/Ar produces a mixture of ground state and excited state iodine atoms, with the excited atoms at 5% of the total[21]. From this information and the total number density of iodine atoms produced by the photolysis (obtained from the laser fluence, the CH_2I_2 density, and the CH_2I_2 absorption cross section at 193 nm) the initial number densities of ground state iodine atoms and excited I* can be determined. For example, for the data of the middle trace in Figure 5A, the initial density of ground state iodine atoms is 3.8×10^{12} cm^{-3} and the density of excited I* atoms is 2.0×10^{11} cm^{-3}. The enhancement of the iodine emission in the presence of $NCl(a^1\Delta)$ is evident in the data from photolysis of NCl_3/CH_2I_2/Ar mixtures. In Figure 5A, for example, the maximum intensity of the I* emission produced from photolysis of this mixture (the top trace) is a factor of 2.8 greater than the initial intensity of the emission from CH_2I_2/Ar alone (determined by extrapolating the exponential decay of the middle trace to time = 0). For this case, then, the densities of excited and ground state iodine atoms at the time of the maximum are 5.6×10^{11} and 3.5×10^{12} cm^{-3}, respectively.

At the maximum, the steady-state expression for the density of excited iodine atoms is

$$[I(5^2P_{1/2})] = k_e[I(5^2P_{3/2})][NCl(a^1\Delta)]/k_q \qquad (7)$$

where k_e is the second order rate constant for excitation of iodine atoms in collisions with $NCl(a^1\Delta)$ and k_q is a first order rate constant for the overall quenching of the excited iodine atoms. This expression can be rearranged to give the density of excited NCl at the steady state, as follows:

$$[NCl(a^1\Delta)] = (k_q/k_e)([I(5^2P_{1/2})]/[I(5^2P_{3/2})] \qquad (8)$$

For the conditions of Figure 5A, $[I(5^2P_{1/2})]/[I(5^2P_{3/2})] = 0.16$ at the steady state. The value of k_e is known[22,23] to be $1.6 \times 10^{-11} cm^3 s^{-1}$ at room temperature, and k_q is determined from either the rise or the decay of the iodine emission signal shown in the figure, depending on which corresponds to the quenching rate. If, for example, the signal decay (360 s^{-1}) were to correspond to the decay rate, then the density of $NCl(a^1\Delta)$ at the steady state would be determined to be 3.6×10^{12} cm^{-3} from eqn. 8. This cannot be the case, though, since for such a density the rate of excitation of the iodine atoms (using $k_e = 1.6 \times 10^{-11}$ $cm^3 s^{-1}$) would be only 58 s^{-1}, far slower than the rate implied by the rise of the signal shown in the figure. On the other hand, if the rise of the signal (at a rate of 5000 ± 500 s^{-1}, determined by a fit to the data) were to correspond to the decay of the excited iodine, then eqn. 8 would suggest the density of $NCl(a^1\Delta)$ at the steady state to be 5.0×10^{13} cm^{-3}. For this density the pseudo-first order rate of excitation of the iodine atoms would be 800 s^{-1}, significantly faster than the observed decay of the emission signal (360 s^{-1}). Since the density of $NCl(a^1\Delta)$ is far greater than the density of ground state iodine

atoms, and the rate of excitation of the iodine atoms is much slower than the rate of quenching of the excited iodine, we infer that the observed decay in fact corresponds to the rate of removal of $NCl(a^1\Delta)$ from the system. Hence the rise of the signal would indeed appear to correspond to the rate of decay of the excited iodine atoms, and the density of excited NCl at the steady state is determined to be 5.0×10^{13} cm^{-3}. This value may be compared to the density of NCl_3 dissociated by the 193 nm laser pulse, 5.1×10^{13} cm^{-3}, to give an apparent quantum yield for the production of $NCl(a^1\Delta)$ of 0.98.

The data shown in Figures 5B and 5C correspond to substantially higher densities of NCl_3 photofragments. A treatment analogous to that described above results in calculated $NCl(a^1\Delta)$ quantum yields of 0.56 and 0.46, respectively, for these data. These

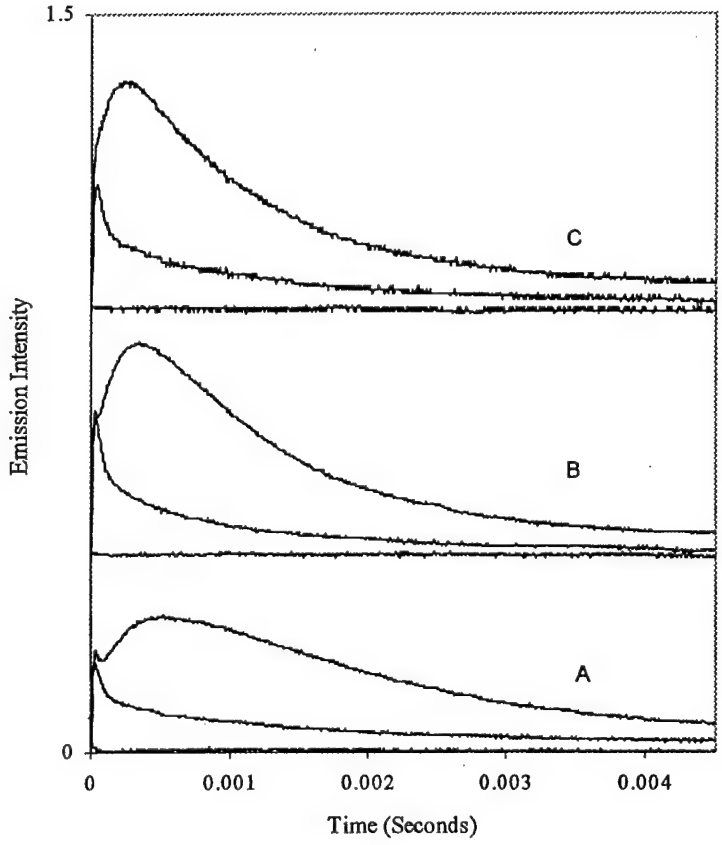

Figure 5. Time profiles of I* emission produced by 193 nm photolysis of mixtures of NCl_3, CH_2I_2, and Ar. (A) lower trace, baseline, middle trace, $[I^*]_0 = 2.0 \times 10^{11}$ cm^{-3}, upper trace $[I^*]_0 = 2 \times 10^{11}$ and density of NCl_3removed by the photolyisis is $5.1 \times 10^{13} cm^{-3}$. (B), lower trace, baseline, middle trace, $[I^*]_0 = 3.3 \times 10^{11}$ cm^{-3}, upper trace, $[I^*]_0 = 3.3 \times 10^{11}$ and density of NCl_3 removed by the photolysis is 1.6×10^{14} cm^{-3}. (C) lower trace, baseline, middle trace, $[I^*] = 3.1 \times 10^{11}$ cm^{-3}, upper trace, $[I^*]_0 = 3.1 \times 10^{11}$ and density of NCl_3 removed by the photolysis is 2.8×10^{14} cm^{-3}.

values are substantially lower than that calculated from the data of Figure 5A, and the difference suggests that quenching of $NCl(a^1\Delta)$ by photofragments in the time between the laser pulse and the maximum of the iodine emission signal may have an effect. Taken together, the three results suggest that the intrinsic quantum yield for production of

$NCl(a^1\Delta)$ at 193 nm is 0.8 ± 0.2. This result certainly implies that demonstration of an iodine laser based on pulsed photolysis of NCl_3/CH_2I_2 mixtures is possible, if the density of NCl_3 in the flow system can be substantially increased.

A detailed description of these results has been published in a recent issue of the Journal of Physical Chemistry[17].

2. Energy Transfer Processes in the NCl_3/I^* System

In a second part of the program, research was performed to investigate the rates of collisional quenching of excited $NCl(a^1\Delta)$ and I^* by NCl_3 and its photoproducts. Since these are species that may be present in abundance in any laser device, the values of these rate constants are quite important. The experiments were based on pulsed photolysis of NCl_3/Ar mixtures at 193 nm and 249 nm. Photolysis at 193 nm generates $NCl(a^1\Delta)$ as described above. Photolysis at 249 nm was used to generate I^* from CF_3I, a well known process[24].

The quenching of $NCl(a^1\Delta)$ was investigated by 193 nm photolysis of NCl_3/Ar mixtures. The time decay of excited NCl was observed in this system via its emission at 1077 nm, such as that shown in Figure 4 above. Time profiles were collected for a variety of NCl_3 densities and exponential decay rates determined from least-squares fits to plots of ln(intensity) vs. time. The rate constant k_1 for quenching of $NCl(a^1\Delta)$ by collisions with NCl_3 is related to the observed rate of decay of the emission signal (λ) according to the following expression:

$$\lambda = k_1[NCl_3] + k_f[\text{fragments}] + k_w \qquad (9)$$

where [fragments] represents the density of the photofragments (excited NCl, Cl_2, and possibly Cl atoms) and k_w is an effective first-order rate constant for quenching of the excited NCl at the cell walls. The value of k_1 was determined from the slope of plots of λ vs. the density of NCl_3. The total pressure was held at a constant value near 1.0 Torr by reducing the flow of Ar diluent as the flow of NCl_3 was increased. This should result in a constant diffusion rate and hence a constant value of k_w. Figure 6 shows a lot of λ vs. the density of NCl_3. While there is considerable scatter in the data, the plot does exhibit a positive slope and from a least squares fit the rate constant for $NCl(a^1\Delta)$ quenching by NCl_3 is determined to be $k_1 = (3.4 \pm 1.7) \times 10^{-13}$ cm^3s^{-1}. The intercept of the plot at $[NCl_3] = 0$ corresponds to the value of k_w for these conditions. Its value, roughly 600 s^{-1}, is reasonable for diffusion at 1.0 Torr of Ar in a 2.54 cm diameter cell, and suggests that quenching of $NCl(a^1\Delta)$ on the stainless steel walls is efficient.

The data shown in Figure 6 were obtained for three different laser fluences ranging from 12 to 50 mJ/cm^2. For this range, the percentage dissociation of the NCl_3 by the laser pulse varies from 6% to 24%. It is apparent from the data that the dissociation percentage has little impact on the observed decay rate, indicating that quenching by second order collision processes among photoproducts (k_f in eqn. 9 above) are indeed unimportant for these conditions. This result argues that the co-product of the photodissociation at 193 nm is likely to be Cl_2 (as indicated in reaction 4) rather than two Cl atoms, as $NCl(a^1\Delta)$ quenching by the atoms is much more rapid[25] than quenching by

Cl_2 and would have been observed as an increase in the observed decay rate with increasing laser fluence.

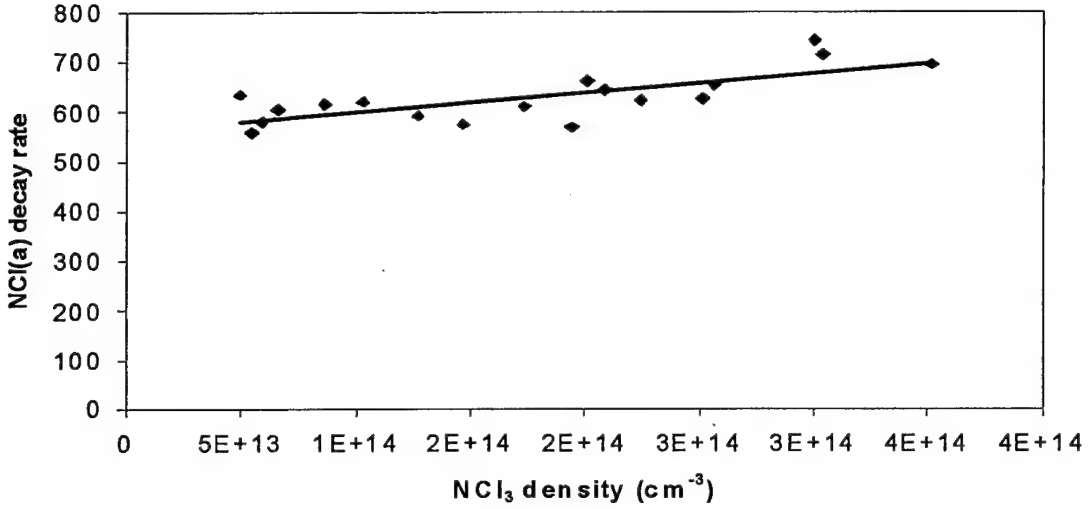

Figure 6. A plot of the exponential decay rate of emission from NCl(a) vs. the initial density of NCl_3. The linear least- squares fit to the slope gives a rate constant k = (3.4 ± 1.7) x 10^{-13} cm^3s^{-1}.

As noted above, photodissociation of NCl_3 at 249 nm produces no excited NCl($a^1\Delta$). Hence, photolysis at this wavelength can be used for measurement of the rate constant for quenching of excited I*($5^2P_{1/2}$) by collisions with NCl_3. For this measurement, a number of experiments were performed in which I* was created by photolysis[24] of CF_3I at 249 nm, in the presence of excess amounts of NCl_3. Emission from the excited iodine atoms at 1315 nm was observed with the cooled Ge detector equipped with a narrow bandpass filter centered on this wavelength. Time profiles of the decay of the I* emission were observed to be exponential in every case and the exponential decay rates were plotted vs. the density of NCl_3 present as shown in Figure 7.

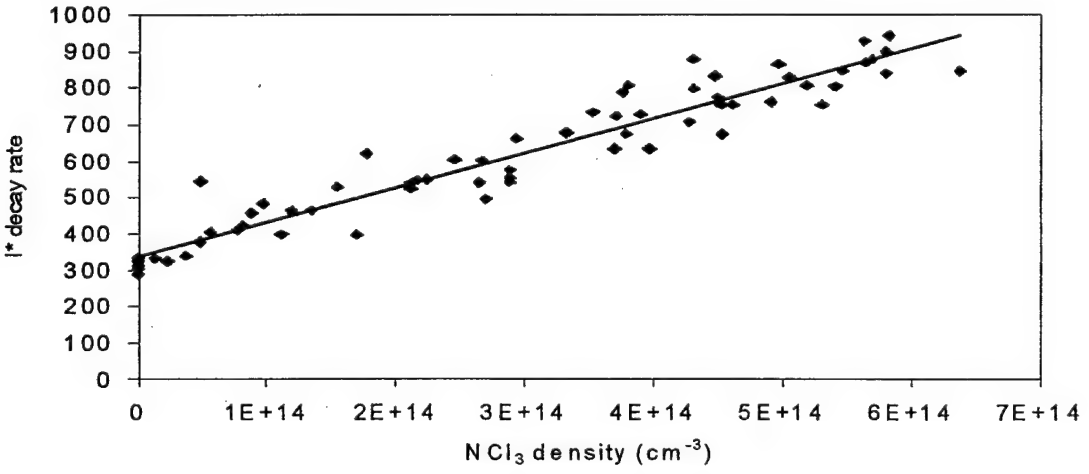

Figure 7. A plot of the exponential decay rate of emission from I*($5^2P_{1/2}$) vs. the density of NCl_3. A Linear least-squares fit to the slope gives a rate constant k= (9.5 ± 2.0) x 10^{-13} cm^3s^{-1}.

The slope of the plot in Figure 7 suggests that the rate constant for I* quenching by NCl_3 is $(9.5 \pm 2.0) \times 10^{-13}$ cm^3s^{-1}. The data shown were taken for four different laser fluences ranging from 12 to 50 mJ/cm^2. These values correspond to dissociation of 1% to 6% of the NCl_3 originally present. Comparison of these four data sets (which have been combined in Figure 7) indicated that the observed I* quenching rate constant did not vary with changes in the fluence. If the doublet dissociation channel (reaction 5 above) is dominant for photolysis at 249 nm, the photolysis products present immediately after the laser pulse are NCl_2 and Cl atoms. Cl atoms are known to efficiently quench I*, with a rate constant[26] of 1.5×10^{-11} cm^3s^{-1} at 300K. Since this value is 15 times greater than the apparent rate constant for quenching by NCl_3 (Figure 7), quenching by Cl atoms should have a significant impact even when just 6% of the NCl_3 is dissociated. The fact that no fluence dependence was observed suggests that the Cl atoms are rapidly removed from the system. If the $[NCl_3] = 0$ intercept of the plot in Figure 7 indicates the value of k_w for I*, the value of k_w for Cl atoms in the same system might be expected to be roughly double this value (from the mass dependence of the diffusion coefficient), or 700 s^{-1}. We note also that Rubtsov[27] has reported the rate constant for reaction of Cl atoms with NCl_3 to be 1.6×10^{-12} cm^3s^{-1}. For this rate constant and the densities of NCl_3 used in the present experiments, Cl atoms would be removed by reaction with the parent NCl_3 at roughly 500 s^{-1} (for mid-range NCl_3 densities). Hence, the combination of removal at the walls and reaction with the parent NCl_3 are such that Cl atoms might well be removed from the system within a few hundred μs after the laser pulse.

3. Pulsed Production of Excited NCl and I* by the H + NCl_2 System

Experiments directed toward the pulsed production of $NCl(a^1\Delta)$ and I* by 193 nm photolysis of NCl_3/CH_2I_2 mixtures were described in section I above. These experiments were extended to the H + NCl_2 system by adding H_2S to the flow as a photolytic source of H atoms. Photolysis of H_2S at 193 nm is known[28] to result in HS + H, with the absorption cross section at this wavelength being 5.8×10^{-18} cm^2, comparable to that for NCl_3. Photolysis of NCl_3 at this wavelength can generate NCl_2 either as a direct fragment by the doublet channel (reaction 5 above) or by reaction of Cl or H atoms with the parent NCl_3.

Photolysis of mixtures of CH_2I_2, NCl_3, and H_2S in Ar diluent at 193 nm produced no additional enhancement of the I* signals shown above (Figure 5), and indeed some reduction in the I* signal was observed. To investigate this matter, mixtures of NCl_3 with H_2S in Ar were photolyzed and the 1077 nm signal from excited $NCl(a^1\Delta)$ observed using the cooled Ge detector equipped with a narrow bandpass filter centered at this wavelength. Figure 8 shows a comparison between these data and the analogous time profile from photolysis of NCl_3 alone in Ar. It is apparent that there is indeed considerable enhancement of the $NCl(a^1\Delta)$ associated with the presence of the H_2S, as shown by the rise of the signal after the photolysis pulse. This is clear evidence of the operation of the pumping reaction

$$H + NCl_2 \rightarrow NCl(a^1\Delta) + HCl \qquad (2)$$

that has been observed in previous discharge-flow experiments[4,8]. This result also suggests that the negative result found when H_2S is added to the CH_2I_2/NCl_3 mixtures reflects either I* quenching by H_2S or pre-reaction between H_2S and CH_2I_2. To test this, a number of experiments were performed in which HI was used as the source iodine atoms rather than CH_2I_2. Figure 9 shows time profiles of the I* emission produced by 193 nm photolysis of $HI/NCl_3/Ar$ and $HI/NCl_3/H_2S/Ar$ mixtures. The trace from $HI/NCl_3/Ar$ once again clearly shows the pumping of I* by $NCl(a^1\Delta)$ (compare with

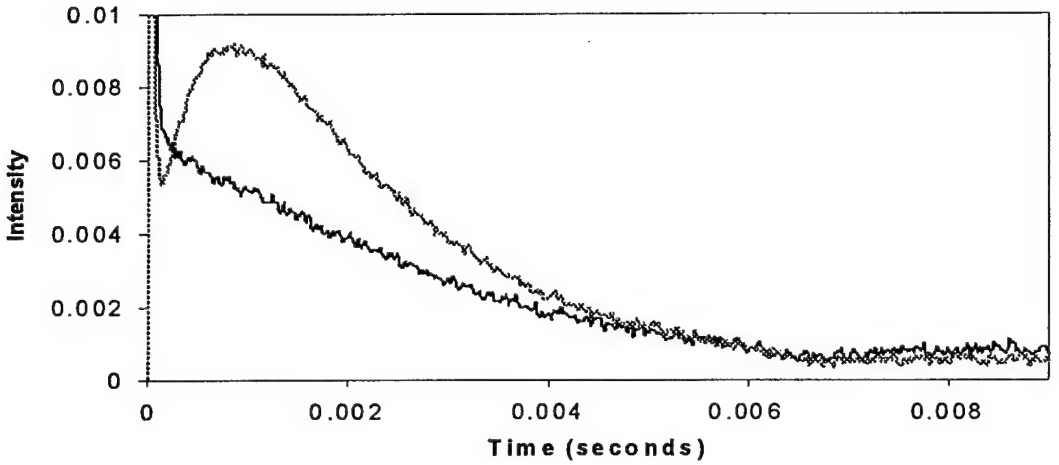

Figure 8. Time profiles of $NCl(a^1\Delta)$ emission . Lower trace, photolysis of NCl_3/Ar at 193 nm; upper trace, photolysis of $NCl_3/H_2S/Ar$ at 193 nm.

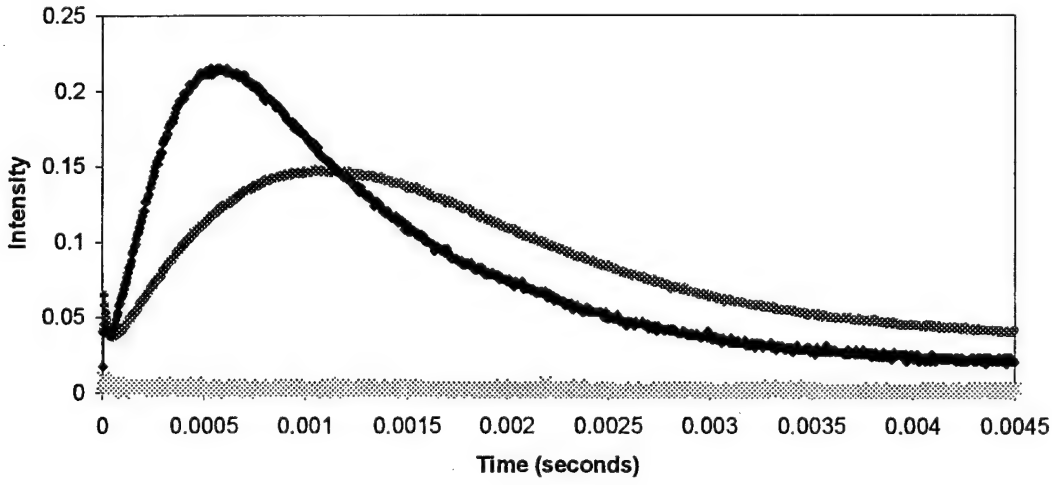

Figure 9. Time profiles of I* emission produced by 193 nm photolysis of NCl_3/Ar (bottom trace), $HI/NCl_3/Ar$ (middle trace), and $HI/NCl_3/H_2S/Ar$ (top trace) mixtures.

Figure 5 above). When H_2S is added to the mixture, though, still more enhancement is observed, along with a clear shortening of the risetime of the emission. We conclude from this result that the negative result noted above was indeed from pre-reaction of the H_2S with CH_2I_2. Further, comparison with the data in Figure 5 (with comparable densities of NCl_3 and laser fluences) indicates that the additional enhancement arising from the presence of H_2S (i.e., production of additional $NCl(a^1\Delta)$ from the $H + NCl_2$ reaction) is such that the I*/I ratio in the system is near 0.25. This value is close to that needed for inversion of the iodine transition, I*/I = 0.33. Hence these results bode very well for the demonstration of a pulsed laser based on this system.

Photolysis of $HI/NCl_3/H_2S/Ar$ mixtures as in Figure 9 above produced a bright blue emission easily visible to the eye. No such emission was observed in the absence of H_2S (see Figure 2 above), and hence experiments were performed in which the spectrum of the new emission was measured. This spectrum, easily identified as the $B\ ^2\Pi \rightarrow X^2\Sigma$ transition in NS, is shown in Figure 11. This transition has been explored[29] by a number of researchers in the past because the short lifetime of the excited state (3μs) and the strong Frank-Condon shift of the transition (giving rise to the progression of bands evident in the spectrum) are appropriate for supporting lasing.

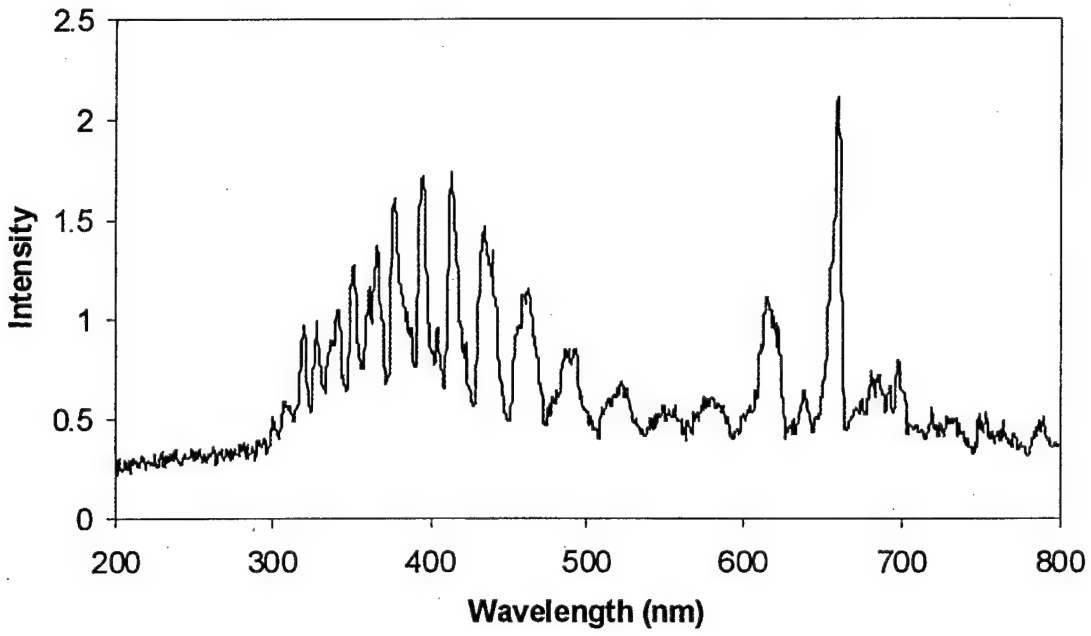

Figure 10. Spectrum of emission from excited NS produced by 193 nm photolysis of $NCl_3/H_2S/Ar$ mixtures. The intense features between 600 and 700 nm correspond to emission from $NCl(b^1\Sigma^+)$, as in Figure 2 above.

It was observed that at faster pulse repetition rates (such that the gas residence time in the cell was longer than the time between pulses), the intensity of the blue emission would oscillate from pulse to pulse -- one pulse intense, the next dim, the next intense, and so on. Further, the time profile of the emission indicated a very fast (electronics limited) rise followed by a decay over roughly 2 μs, suggesting that the excited NS is produced as a direct photolysis fragment of some precursor rather than by collisions. The oscillatory nature of the emission suggests that the precursor is generated by chemistry initiated by one pulse, then is itself photolyzed (producing the excited NS) by the next

pulse. For example, HS might react with NCl_2 (both produced by the first 193 nm laser pulse) to generate an $HSNCl_2$ molecule, which would eliminate HCl to produce ClNS. This molecule, which is similar to the well-known species ClNO, might well be photolyzed to produce excited NS. Interestingly, ClNS has not been observed in the gas phase.

Part II. Low Energy Deposition of BN Thin Films

Our work in this area represents the continuation of a project begun under the aegis of a previous AFOSR grant[30]. It is based on the dissociation of an energetic BN precursor, $B(N_3)_3$, for which a facile gas phase synthesis has been developed[12]. Our previous work explored $B(N_3)_3$ dissociation by thermal decomposition, photolysis, and collisions with energetic metastable species. In particular, dissociation by collisions with $N_2(A^3\Sigma_u^+)$ metastables was found to produce thick, hard amorphous boron nitride films with a B:N ratio near unity[14]. Matrix isolation studies performed in the laboratory of Professor J.V. Gilbert[31] identified the linear molecule NNBN as the product of $B(N_3)_3$ photodissociation, and it has been speculated that thin films of BN may be formed by self-assembly of these molecules.

All of the films produced in this previous work were found to be amorphous, and it was concluded that while the energy liberated by the dissociation of $B(N_3)_3$ was sufficient to drive the chemistry underlying the production of hexagonal BN, it occurred largely in the gas phase and did not provide the surface mobility needed for the generation of polycrystalline film structures with long range order[14]. Indeed, this system appears to provide a unique situation in which the chemical and physical aspects of the film deposition mechanism are well separated from one another. Although the initial B:N ratio in these films was near 1:1, the films were amorphous and contained substantial amounts of oxygen. Further, the films degraded rapidly upon exposure to air, a phenomenon thought to be associated with the formation of hydrides as atmospheric moisture saturated the films via their extensive pore structure. The formation of these hydrides was observed by the growth of a broad and intense high frequency feature ($\approx$3400 cm^{-1}) in the infrared absorption spectra of the films. When this occurred (within hours of exposure to air), the films became visually cloudy and adhered poorly to the substrates used (silicon and sapphire).

Consequently, research performed in the present program addressed this second part of the issue, the physical formation of hard, dense crystalline or polycrystalline films. The research involved film deposition by plasma dissociation of $B(N_3)_3$. In addition, a preliminary investigation of the molecular mechanism of film formation was performed based on both experimental and theoretical methods.

1. Plasma Deposition of BN Thin Films

Plasma-assisted film deposition, with the plasma both dissociating the azide precursor and providing enhanced surface mobility to the chemical precursors of the films, has the potential to produce films with substantially improved characteristics. A low energy dc discharge was added to the film deposition apparatus described previously[14] such that an

Ar plasma was produced and directed to the substrate surface. The substrate (either Si 100, sapphire, or Ni 100) was mounted on a stage that could be heated to temperatures of several hundred degrees. $B(N_3)_3$ was produced by the stoichiometric gas phase reaction[12] between BCl_3 and HN_3 and was admitted to the deposition chamber by a small injector such that two plumes, one the Ar plasma and the other the $B(N_3)_3$/ Ar flow, mixed with one another over the substrate surface. The entire system was enclosed within a stainless steel vacuum chamber pumped by a 6.0 inch diffusion pump and cryotrap.

Plasma deposition experiments were performed with Si substrates held at temperatures from ambient to 400°C. The films generated were very clearly different from those previously produced in that they did *not* become cloudy on exposure to lab air, and there was no evidence of hydride formation. Figures 11a and 11b show the IR spectra of such a film taken immediately after deposition and after exposure to lab air for *two months*. There are no IR features in either spectrum other than those[32] associated with sp^2 -bonded (hexagonal) BN, at 1390 and 800 cm^{-1}. There is no evidence of a hydride feature (typically at frequencies above 3000 cm^{-1}) in either spectrum.

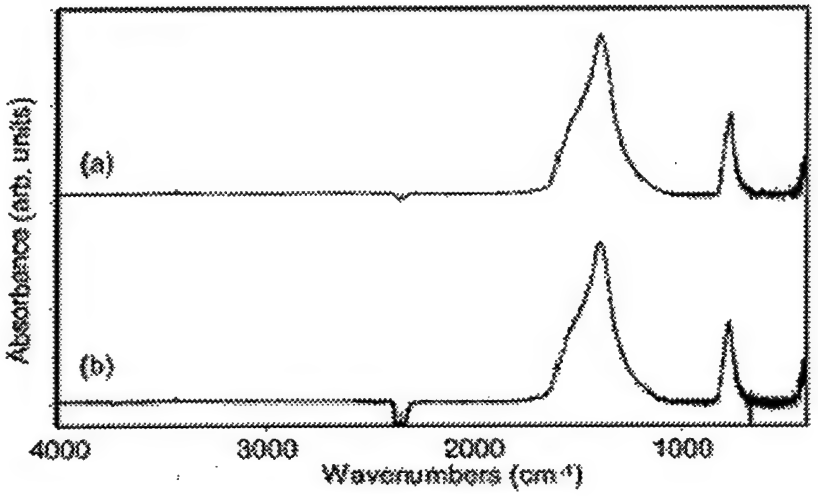

Figure 11. Infrared spectrum of films deposited on silicon by plasma dissociation of $B(N_3)_3$.
(a) Spectrum of film immediately after deposition, (b) Spectrum of film 2 months after deposition.

This result was supported by measurements of x-ray photoelectron spectra of the films. Table I shows the chemical composition of a typical film determined from the XPS data, at the surface and after an argon ion etch to reveal interior features. The B:N ratio at the surface is very nearly 1:1, and although some oxygen is present this is likely associated with contamination of the surface by lab air. In fact the argon ion etch removed most of the oxygen, showing that there is rather little in the interior of the film . The slightly larger B:N ratio in the interior (about 1.2:1.0) reflects preferential loss of N atoms in the etch.

Although XRD measurements of the films showed no evidence of crystallinity, x-ray reflectivity measurements did indicate that the film density was 2.5 g/cm^3, quite large for an sp^2 - bonded film. Measurements with a stylus profilometer indicated that the films were on the order of 100 nm in thickness, perhaps too thin for our XRD measurements to reveal crystallinity. The films were much more adherent than those made by

photodissociation or collisional dissociation in the gas phase, and were not removed from the substrates by vigorous washing or rubbing. SEM images of the films showed no indication of grain structure up to magnifications exceeding 100,000. Interestingly, the SEM images revealed the formation of long, linear fissures after scoring with a stylus, certainly suggestive of crystallinity.

Table I. XPS Elemental Analysis of BN Film from Plasma Deposition

	Atomic Concentration (%)[a]				
	B	N	C	O	Cl
Surface	33.37	31.91	22.05	12.67	
Interior	51.2	41.87	1.44	3.66	1.84

(a) The atomic concentrations are normalized to 100% in each spectrum

A particularly interesting characteristic of these films is that they show *no* indication of cubic (sp^3 - bonded) structure, even under conditions (substrate temperature, plasma current density and ion momentum) for which some formation of sp^3 BN is expected[32]. Ordinarily, this would be observed by the presence of a feature[33] at 1080 cm^{-1} in the IR spectrum, and data such as that shown in Figures 12a and 12b show no such features. To further investigate this issue, a number of experiments were performed in which single crystal Ni (100) was used as a substrate. This surface has an excellent lattice match with sp^3 - bonded BN, and a number of authors[34] have reported preferential formation of cubic structures on nickel substrates. Figure 12 shows a reflectance IR absorption

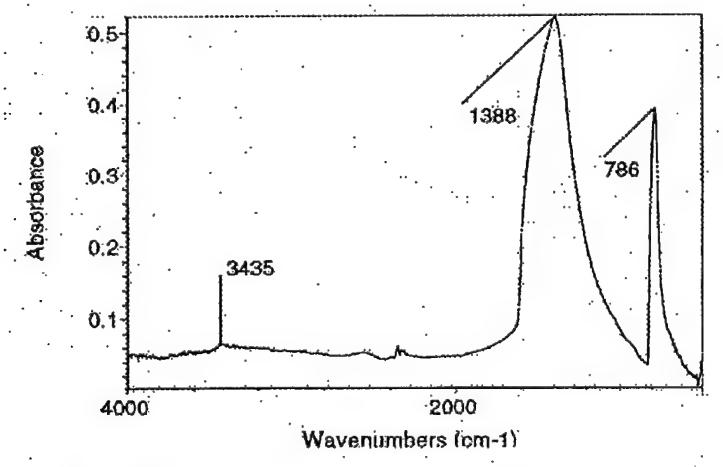

Figure 12. Reflectance IR absorption spectrum of a BN film on Ni(100) deposited by plasma deposition of $B(N_3)_3$

spectrum taken of a BN film on nickel (100) deposited by plasma dissociation of $B(N_3)_3$. Once again, the spectrum indicates the presence of only sp^2 - bonded BN. XPS analysis of such films indicated that they had very good chemical purity, quite similar to that of the films grown on silicon. Although there was no evidence of chemical degradation in lab air, the films on nickel were clearly less adherent. SEM images of such films

indicated peeling from the substrate, suggestive of poor bonding. This result certainly supports the conclusion that the films are comprised largely of sp^2 - bonded BN, which has a poor lattice match with the nickel surface.

A detailed description of the plasma-assisted deposition of BN films from $B(N_3)_3$ has recently been published in Thin Solid Films[35].

2. Molecular Mechanism of BN Film Formation

In 1998, Professor J.V. Gilbert and co-workers in our department at the University of Denver were able to trap $B(N_3)_3$ in a low temperature argon matrix and identify its photodissociation products[31]. The principal fragment observed was linear NNBN, presumably formed from rearrangement of a trigonal BN_3 species produced by loss of three N_2 molecules from $B(N_3)_3$. NNBN is isoelectronic to cyanogen and calculations[31] at the CCSDT level of theory with an extensive basis set revealed it to have an oscillating charge distribution akin to that in isocyanogen (NCNC). From this result, it was inferred that self-assembly of these NNBN fragments into trimers could easily generate six-member BN ring structures, i.e., hexagonal (sp^2 - bonded) BN. Calculations of the lowest energy path for this self-assembly process were described in a previous AFOSR report[30]. In short, a mechanism based on formation of dimers, then trimers, followed by ring closure was found to have a substantially attractive potential for each step. These calculations were done using DFT methods. During the current reporting period, this computational work was extended to include calculations of the vibrational frequencies of a number of BN ring structures including the NNBN trimer and the trimer less one, two, and three N_2 molecules. The results of these calculations, done at theB3LYP/6-31g* level of theory, are shown in Table II. In each case, the most intense IR feature falls at a frequency near 1600 cm^{-1} and is associated with a ring stretching mode.

The self-assembly of NNBN fragments into six-member BN rings in the gas phase (i.e., before deposition on the substrate) could be the reason that *no* sp^3 - bonded BN is observed in plasma deposition from $B(N_3)_3$. To test this hypothesis, a number of experiments were performed in which $B(N_3)_3$ was injected into an argon plasma in a discharge-flow reactor. A pinhole probe sampled the gas mixture in the interaction region and the species extracted from the flow were deposited onto the cold window of a low temperature matrix isolation apparatus. If NNBN or its self-assembly products are formed in the gas phase, their presence should be evident in the IR spectra of these matrices. Figure 13 shows a series of spectra of the 1600 cm^{-1} region recorded in such an experiment. Clearly, a feature in this region (at 1640 cm^{-1}) is observed to grow in after the discharge is turned on. Given the data in Table II, this result strongly indicates the formation of six-member BN ring structures in the gas phase. Figure 14 shows the intensity of the 1640 cm^{-1} feature and that of the feature at 2157 cm^{-1} (the N_3 stretching vibration in $B(N_3)_3$) as a function of time. These data show that the deposition of $B(N_3)_3$ decreases when the discharge is turned on, at which point the linear growth of the 1640 cm^{-1} feature begins. When the discharge is turned off, growth of the 1640 cm^{-1} feature ceases and deposition of $B(N_3)_3$ begins again. Hence the 1640 cm^{-1} feature seems to be clearly associated with dissociation of $B(N_3)_3$ in the plasma. Once again, this suggests self-assembly of $B(N_3)_3$ dissociation fragments into BN rings in the gas phase. This

result certainly offers one explanation for the absence of sp^3 - bonded BN in our films, and suggests that the deposition of films with cubic structure will require that $B(N_3)_3$ be dissociated exclusively on the substrate surface.

Table II. Frequencies[a] and Intensities[b] of vibrations of BN Ring Structures

B_3N_3		B_3N_5		B_3N_7		B_3N_9	
Freq.	Intensity	Freq.	Intensity	Freq.	Intensity	Freq.	Intensity
484.3	0.0	86.3	0.2	67.5	1.1	18.2	0.3
484.4	0.0	110.2	0.1	70.5	0.4	20.6	0.1
535.2	66.4	201.7	0.7	89.0	0.0	21.5	0.1
591.4	40.7	288.1	2.1	115.5	1.1	37.7	0.0
591.6	40.8	428.8	2.3	123.5	1.6	38.9	0.0
798.7	0.0	487.0	0.0	134.8	4.7	43.7	0.0
1023.9	0.0	521.9	30.7	268.5	0.0	55.7	0.1
1028.0	28.1	546.4	45.3	281.5	4.5	58.7	6.9
1028.3	28.2	560.6	61.1	377.5	1.9	59.2	7.0
1378.8	0.0	582.2	30.1	442.1	1.6	92.0	95.7
1618.3	**489.3**	763.7	2.4	514.3	11.0	103.0	0.0
1618.4	**485.8**	936.3	38.0	518.6	106.1	103.5	0.0
		1033.5	16.0	524.1	66.2	136.1	0.0
		1052.6	36.5	563.1	0.0	137.3	0.0
		1299.8	103.4	598.0	44.0	188..2	0.0
		1520.7	279.6	717.8	0.0	498.9	0.0
		1644.6	**471.6**	921.2	13.7	499.4	0.0
		2346.8	44.0	1010.2	93.5	551.8	58.9
				1055.9	16.7	564.2	120.1
				1311.8	69.1	564.9	120.7
				1436.0	356.3	770.7	0.0
				1623.0	**346.6**	1004.8	0.0
				2340.1	106.9	1023.5	102.5
				2342.0	19.8	1024.0	101.5
						1376.0	0.0
						1602.1	**533.6**
						1603.0	**533.7**
						2371.1	1.1
						2371.2	1.4
						2371.2	0.4

(a) Calculated frequencies in cm^{-1}, scaled by a factor of 0.9613
(b) Intensities in arbitrary units

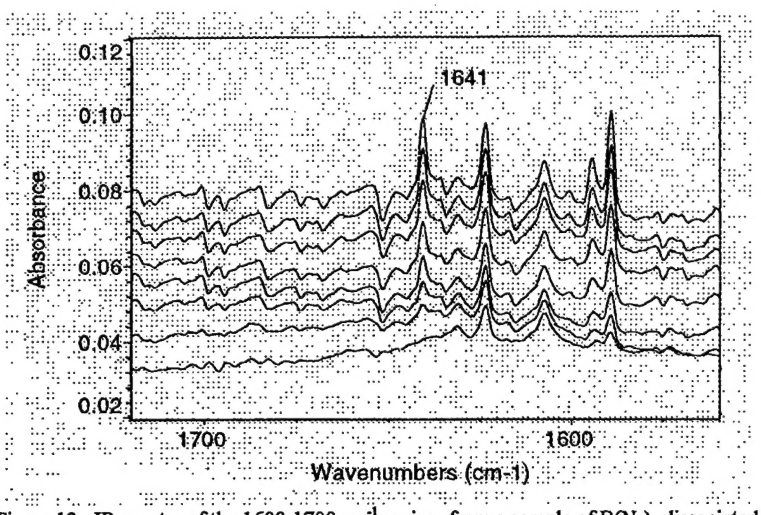

Figure 13. IR spectra of the 1600-1700 cm^{-1} region, from a sample of $B(N_3)_3$ dissociated in a discharge through Ar. The bottom spectrum was taken earliest, the top spectrum latest

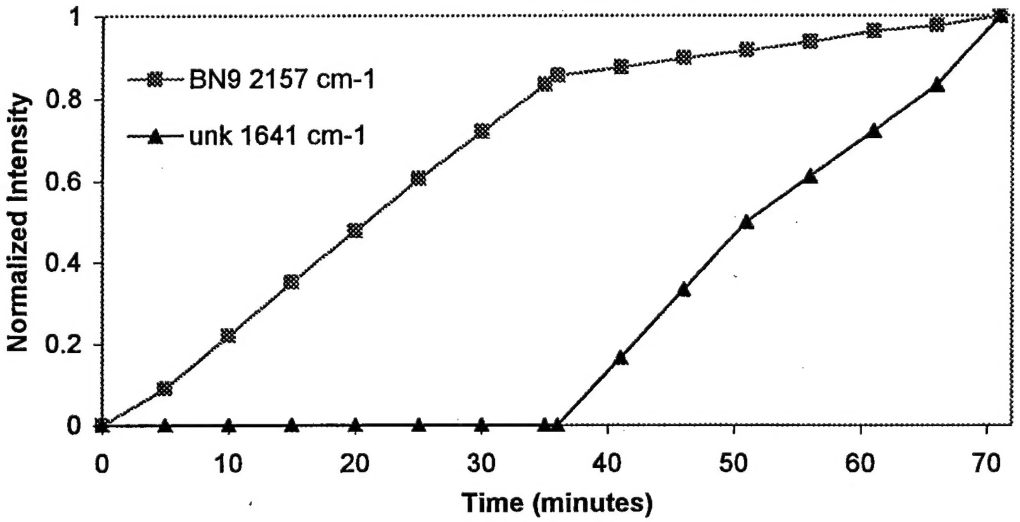

Figure 14. Intensities of the 1640 and 2157 cm^{-1} features as a function of time.

CONCLUSIONS

The experiments described above have demonstrated conclusively that NCl_3 is an effective source of excited $NCl(a^1\Delta)$, either by reaction with hydrogen atoms or by photodissociation at 193 nm. In the latter case, we note that 193 nm lies well within the most intense UV absorption absorption feature of the molecule, and that there may well be a substantial photochemical yield of $NCl(a^1\Delta)$ throughout the 190-230 nm region. If so, an I* laser based on photodissociation of NCl_3 might well be demonstrated by pulsed

flash photolysis methods. This would likely require the production of densities of gas phase NCl_3 substantially greater than those used in the present experiments.
The energy associated with this UV band in NCl_3 is near that of a number of electronically excited metastables, including triplet states of N_2 and rare gas atoms. It is interesting to speculate whether excited NCl might be produced by collisions of NCl_3 with such metastables, suggesting the possiblility of a pulsed discharge-pumped AGIL. Gershanovich and Gilbert[36] have published the results of a preliminary investigation of this possibility.

Collisional quenching of both $NCl(a^1\Delta)$ and I* by NCl_3 and its photoproducts appears to be relatively slow. This result agrees with previous observations of the compatibility of excited I* with the H/NCl_3 chemical system[8], and bodes well for good scaling of a cw laser device. Further information concerning the temperature dependence of the rate constants reported in this work is needed, as the operating temperature of current subsonic AGIL devices[6] is several hundred °C. The maximum densities of excited $NCl(a^1\Delta)$ produced in these pulsed experiments were near 10^{14} cm^{-3}, more than an order of magnitude greater than those achieved in previous studies of the H/NCl_3 system in discharge-flow reactors[4,8]. It is clear that this amine system is compatible with the generation of I* at these higher densities, and further scaling certainly appears to be possible.

$B(N_3)_3$ is a very good chemical source of BN. Plasma-assisted deposition of BN from $B(N_3)_3$ produces films that are hard, adherent, and stable with B:N ratios near unity. These films exhibit no crystallinity, though, a result likely associated with the molecular mechanism of $B(N_3)_3$ dissociation and BN generation. The present results suggest that dissociation of the azide to NNBN leads to the production of hexagonal B_3N_x ring structures in the gas phase by rapid self-assembly of these fragments prior to surface deposition. Hence, the species actually deposited on the substrate surfaces may well be hexagonally bound nanoparticles of BN, such that some form of additional energy deposition on the surface would be required for annealing to produce a polycrystalline film. Indeed, it would be reasonable to investigate the possiblility of using $B(N_3)_3$ as a source of BN nanoparticles, using conventional methods[37] for the production of such nanoparticles from CVD precursors.

REFERENCES

1. W.E. McDermott, N.R. Pchelkin, D.J. Benard, and R.R. Bousek, Appl. Phys. Lett., **32**, 469 (1978).
2. See for example D.J. Benard, W.E. McDermott, N.R. Pchelkin, and R.R. Bousek, Appl. Phys. Lett., **34**, 40 (1979).
3. A.T. Pritt and R.D. Coombe, Int. J. Chem. Kinetics, **12**, 741 (1980).
4. D.B. Exton, J.V. Gilbert, and R.D. Coombe, J. Phys. Chem., **95**, 2692 (1991).
5. A.J. Ray and R.D. Coombe, J. Phys. Chem., **99**, 7849 (1995).
6. T.L. Henshaw, G.C. Manke II, T.J. Madden, M.R. Berman, and G.D. Hager, Chem. Phys. Lett., **325**, 537 (2000).
7. P. Cadman, J.C. Polanyi, and I.W.M. Smith, J. Chem. Phys., **64**, 111 (1967).
8. R.W. Schwenz, J.V. Gilbert, and R.D. Coombe, Chem. Phys, Lett., **207**, 526 (1993).

9. See for example J.A. Rodriguez, C.M. Truong, J.S. Corneille, and D.W. Goodman, J. Phys. Chem., **96**, 334 (1992).
10. See for example S.P. Murarka, C.C. Chang, D.N.K. Wang, and T.E. Smith, J. Electrochem. Soc., **126**, 1951 (1979).
11. G.B. Stringfellow, J. Crystal Growth, **58**, 194 (1983).
12. R.L. Mulinax, G.S. Okin, and R.D. Coombe, J. Phys. Chem., **99**, 6294 (1995).
13. Synthesis and Properties of Boron Nitrides, in Materials Science Forum (Aedermannsdorf, Switzerland, J.J. Pouch and A Allerevitz, eds.) **54/55**, 1990.
14. K.R. Hobbs and R.D. Coombe, J. Appl. Phys., **87**, 4586 (2000).
15. "Advanced High-Energy Closed Cycle Iodine Chemical Lasers", AFOSR grant no. F49620-02-1-0331.
16. J.V. Gilbert, X.-L. Wu, D.H. Stedman, and R.D. Coombe, J. Phys. Chem.,**91**, 4265 (1987).
17. R.D. Coombe, J.V. Gilbert, S.P. Beaton, and N. Mateljevic, J. Phys. Chem. A, **106**, 8422 (2002).
18. T.C. Clark and M.A.A. Clyne, Trans. Faraday Soc., **65**, 2994 (1969).
19. A.T. Pritt, Jr. D. Patel, and R.D. Coombe, J. Mol. Spectrosc., **87**, 401 (1981).
20. A.T. Pritt, Jr., D. Patel, and R.D. Coombe, J. Chem. Phys., **75**, 5720 (1981).
21. W.H. Pence, S.L. Baughcum, and S.R. Leone, J. Phys. Chem., **85**, 3844 (1981).
22. T.L. Henshaw, S.D. Herrera, and L.A. Schlie, J. Phys. Chem. A, **102**, 6239 (1998).
23. A.J. Ray and R.D. Coombe, J. Phys. Chem., **97**, 3475 (1993).
24. T.F. Hunter, S. Lunt, and K.S. Kristjansson, J. Chem. Soc. Faraday Trans. 2, **79**, 303 (1983).
25. G.C. Manke II and D.W. Setser, J. Phys. Chem., **102**, 7257 (1998).
26. M.D. Burrows, J. Chem. Phys., **81**, 3546 (1984).
27. N.M. Rubtsov, Mendeleev Comm., 173 (1998).
28. W.G. Hawkins and P.L. Houston, J. Chem. Phys., **73**, 297 (1980).
29. T.L. Henshaw, A.P. Ongstad, and R. Lawconnell, J. Phys. Chem., **94**, 3602 (1990).
30. R.D. Coombe, Final Report, AFOSR grant no. F49620-97-1-0036.
31. I.A. Al-Jihad, B. Liu, C.J. Linnen, and J.V. Gilbert, J. Phys. Chem. A, **102**, 6220 (1998).
32. D.J. Kester and R. Messier, J. Appl. Phys., **72**, 504 (1992).
33. See for example K.F. Chan, C.W. Ong, and C.L. Choy, J.Vac. Sci. Technol. A, **17**, 3351 (1999).
34. Z. Song, F. Zhang, Y. Guo, and G. Chen, Appl. Phys. Lett., **65**, 2669 (1994).
35. K.R. Hobbs and R.D. Coombe, Thin Solid Films, **402**, 162 (2002).
36. Y. Gershanovich and J.V. Gilbert, J.Phys. Chem, **101**, 840 (1977).
37. See for example X. Peng, L. Manna, W. Yang, J. Wickham, E. Scher, A. Kadavanich, and A.P. Alivisatos, Nature, **404**, 59 (2000).